PUSHING THE LIMITS OF SHORT PERIOD PERMANENT MAGNET UNDULATORS

J. Bahrdt, ANL, Argonne, Il 60439, USA, on leave from HZB, 12489 Berlin, Germany

Abstract

Short period undulators to be used as FEL radiators permit lower electron energies and, thus, reduced linac and undulator lengths. The first X-ray FEL facility based on in-vacuum permanent magnet undulators has gone into operation, already (SACLA). Another in-vacuum undulator based X-FEL is planned (SWISS-FEL). The in-vacuum undulators have period lengths of 18mm (SACLA) and 15mm (SWISS-FEL), respectively. In the future the period length will be pushed further into the sub-cm regime. The technical challenges of such devices will be discussed: New magnet materials such as PrFeB-magnets are employed. They show their superior characteristics at cryogenic temperatures. Sophisticated pole geometries are under discussion. Geometric and magnetic tolerances become tighter and the construction and shimming concepts have to be revised. A redesign of magnet measurement systems is needed as well. Recently, a 9mm period length 20 period cryogenic undulator has been built in a collaboration of Ludwig-Maximilian-University Munich and Helmholtz-Zentrum Berlin. The potential and the challenges of sub-cm permanent magnet undulators will be illustrated based on first results from this prototype.

INTRODUCTION

The synchrotron radiation of 3rd generation light sources is produced predominantly from permanent magnet undulators and this is the case also for all operational or planned soft and hard X-ray free electron lasers. Planar permanent magnet undulators are used for more than 30 years. Variably polarizing devices of the APPLE II type have become a standard source at many light sources [1]. Quasi-periodic structures have been developed for the suppression of higher harmonics at the sample and several quasi-periodic APPLE structures are in operation [2-4]. Planar in-vacuum undulators have been developed at SPRING-8 and are used in many synchrotron radiation facilities.

Alternatively, electromagnetic or superconducting devices can be used. A superconducting undulator (SCU) is in operation at ANKA since 2005 [5] and further SCUs are under construction at ANKA [6] and the APS [7]. Undulators based on Nb_3Sn have been studied and high temperature superconductor tapes for the application in small period undulators are considered [8]. A few electromagnetic undulators or electromagnet permanent magnet hybrids are used in the low photon energy (large period length) range. In most cases, however, permanent magnet undulators are the only choice and this will be the case for the next years. Permanent magnets can be modelled as blocks carrying surface currents of at least 10kA/cm. Electromagnets cannot compete due to cooling problems, when the dimensions become small. SC undulators are promising but the technology is still under development.

Currently, the development in permanent magnet undulator technology concentrates on planar cryogenic permanent magnet undulators based on NdFeB or PrFeB with period lengths of about 16mm and on small period small gap devices with period length below 10mm. Another goal of development is the field enhancement of variably polarizing devices such as APPLE III [9] (out of vacuum) or DELTA [10] (in-vacuum) undulators.

Storage ring undulators have to provide enough transverse space for injection and a large horizontal good field region in order to enable high injection efficiencies. The magnetic gap must be large enough not to interfere with storage ring operation and to avoid radiation damages. The requirements for single pass devices are different and the undulator design has to be adopted appropriately. A large transverse aperture or a good field region of typical 1-2cm is not needed and the magnetic gap is only limited by wakefield effects.

In this article we concentrate on the development issues of planar small period small gap devices without addressing specific applications though keeping in mind 2nd harmonic afterburners and FEL radiators for laser plasma sources.

MATERIAL DEVELOPMENT

In the 20th century the energy product of permanent magnets increased by more than two orders of magnitude. Today high performance permanent magnets are either of the Sm_2Co_{17} ($SmCo_5$) or the $Nd_2Fe_{17}B$ type. The energy product $(BH)_{max}$ is not expected to increase much further in the future. At room temperature the theoretical limit for $Nd_2Fe_{17}B$ is 509kJ/m^3, and 469kJ/m^3 has been achieved, already, though, commercially available grades have lower values. The gap of less than 10% to the theoretical limit is due to the difference in maximum remanence which is given by:

$$B_r(20°C) = B_{r-sat}(20°C) \cdot \frac{\rho}{\rho_0} \cdot (1 - V_{nonmagnetic}) \cdot f_\varphi$$

$$f_\varphi = \cos(\varphi)$$

$$\varphi = \arctan\left(2\frac{B_{r-perp}}{B_{r-par}}\right)$$

For $Nd_2Fe_{14}B$ magnets the relevant parameters are given in [11-12]: The small deviation from the single crystal density, $\rho/\rho_0 > 0.995$, is achieved with the so-called liquid phase sintering. A high alignment factor of $f_\varphi > 0.98$ is the result of a sophisticated pressing procedure

ISBN 978-3-95450-117-5

where the timing of the magnetic field for grain alignment is a crucial parameter. The amount of non-magnetic material is typical below 4%.

Though, today's permanent magnets achieve 90% of the theoretical energy product, the coercivity H_{cj} (magnet stability) is still an order of magnitude below the theoretical limit, which is known for many decades as Brown's paradoxon [13]. $Nd_2Fe_{17}B$ magnets are of the nucleation type. After magnetization the whole grain of a few µm in size represents a single domain. Once, a part of the grain flips, the whole grain reverses magnetization. Kronmüller [14] discusses quantitatively the influence of inhomogeneities on the coercivity such as: i) non-magnetic extended grains between magnetic grains, ii) misoriented grains, iii) missing grain boundary surfaces resulting in large grains, iv) extended transition regions of tilted crystal structures between grains. Extensive experimental investigations related to the enhancement of coercivity have been done at many places during the last years, e.g. the relation between grain size and coercivity has been studied in detail [15]. In the grain size range of a few µm the coercivity decreases proportional to $(size)^{-0.45}$ and limiting the grain size growth during sintering is one of many essential aspects. The complex microstructure of sintered magnets will require further investigations and major improvements are not expected in the near future.

There are, however, other strategies to enhance the coercivity. Usually, the magnets can be stabilized with the addition of Dysprosium within the grains which increases the coercivity on one hand, but lowers the remanence on the other hand. Shin-Etsu developed a new process which they call the two-alloy-method. The two alloys with different melting points are the bulk grain material, and components of the boundary material embedding the grains, respectively. The latter one has the lower melting point. Adding Dysprosium to this alloy provides a slight concentration of Dysprosium close to the boundaries which alleviates the detrimental impact to the remanence though the Dysprosium still penetrates deeply into the grains at typical sintering temperatures between 1050 and 1100K.

Already 10 years ago the so-called **G**rain **B**oundary **D**iffusion process (GPD) has been described by Park et al. [16]: After sintering the magnets are coated with heavy rare earths (HRE) such as Dysprosium or Terbium and, then, heat-treated. On a short time scale the HRE diffuses along the liquid Nd-enriched boundary into the material and on a longer time scale partly into the solid grains, forming thin HRE enriched shells around the grains. In the last ten years several companies developed this process further and today GPD-magnets are available for specific applications. The material shows an average increase of coercivity of about 3kOe without sacrificing remanence. Microscopic studies show a sharp concentration of HRE at the boundaries and no HRE inside the grains.

Nakamura et al. [17] investigated the depth profile of the coercivity in detail. After sintering the magnets are dipped into a suspension of Tb fluoride (Dy fluoride can be used as well) before the 10-20h heat treatment between 800-900°C starts. Cutting the magnets afterwards into slices, the measurement of the slices indicate a depth scaling of the coercivity of

$$\Delta H_{cj} = Ae^{-x^2/d^2}$$

with x being the distance to the surface. At the surface an increase in coercivity of up to 700kA/m is observed where the increase A depends linearly on the thickness of the HRE surface layer. The penetration depth is about $d=2.2mm$ and it depends neither on the thickness of the surface layer nor on the diffusion time.

The results demonstrate that GPD is of particular interest for small period devices with thin magnets where the process is most effective. However, also larger magnets may benefit from GPD since often only the edges and corners of magnets are exposed to high reverse fields. The magnets of the SWISS-FEL undulator Aramis will be based on GPD-material [18].

CRYOGENIC UNDULATORS

In 2004 T. Hara et al. suggested so-called cryogenic undulators where the magnets are operated at 150K [19]. The thermal coefficients of the remanence and the coercivity of $Nd_2Fe_{17}B$, -0.1%/K and -0.6%/K, respectively, raise the performance of undulators operated at lower temperatures. Additionally, another magnet grade with a lower coercivity can be used because the magnets do not have to be baked and they gain enough radiation stability when they are cooled.

The optimum operation temperature for $Nd_2Fe_{17}B$ magnets is 135K. Below this temperature a spin reorientation [20] occurs which lowers the remanence. This is caused by the temperature dependence of the anisotropy constants K_1 and K_2 which determine the crystalline anisotropy energy via:

$$E = K_1 sin^2(\vartheta) + K_2 sin^4(\vartheta) \quad (1)$$

where ϑ is the angle between the axis of magnetization and the crystal axis. Above 135K E has a minimum at $\vartheta = 0$ and below 135K the energy minimum shifts towards larger angles with

$$\vartheta = \text{asin}(\sqrt{-K_1/2K_2}$$

for $-K_1 < 2K_2$ reaching 26° at 4.2K.

$Nd_2Fe_{17}B$ based cryogenic undulators have been built at the ESRF [21-22], by ADC for NSLS [23], by SPRING-8 for the Swiss Light Source [24] and by DANFYSIK for DIAMOND [25]. The ESRF device and the SLS device are in operation. The cryo-ready undulator at NSLS has not been cooled yet.

All these devices are cooled with liquid nitrogen. This implies that the structures have to be heated actively in order to keep the magnets above the spin reorientation temperature. A careful mechanic design is required to avoid thermal gradients and an unintentional bending of

ISBN 978-3-95450-117-5

the magnet girders. This specific problem can be avoided if the $Nd_2Fe_{17}B$ magnets are replaced by PrFeB magnets which do not show a spin reorientation. In reality, the Nd is not completely substituted by Pr, however, we will use the term PrFeB having in mind $(Nd_xPr_{1-x})_2Fe_{17}B$. The magnets are cooled with liquid N_2, and the final temperature is stable without active compensation. PrFeB magnets have nearly the same magnet properties as $Nd_2Fe_{17}B$, but the availability is smaller since the fields of application are limited. Recently, a PrFeB based undulator has been built at SOLEIL and the installation is planned for end of 2011 [26-28]. Another 8 period PrFeB based undulator with a period length of 14.5mm has been built at the NSLS. It has been measured in liquid N_2 and liquid He cryostates [29] and the data agree with simulations on the %-level.

Principally, PrFeB magnets can be cooled even further if cryocoolers are used. The remanence and coercivity are still increasing, though, the temperature coefficients converge to zero at about 10K. The gain in ccoercivity between 135K and 10K is remarkably high (20kOe). However, this should not be misinterpreted as a significant gain in stability against radiation damage Reversible radiation damages as observed at the ESRF [30] or the APS [31] are understood as a local heating of parts of the magnet above the Curie temperature. Radiation hardness is only achieved by lowering the operation temperature whereas the increased coercivity does not provide an extra benefit. If a particle shower hits a magnet the coercivity increases instantaneously with the local temperature rise. The grain which is hit will get demagnetized immediately before the energy can dissipate into the surrounding material. A reasonable figure of radiation hardness is the energy which can be dumped into the magnet before it reaches the Curie temperature. Fig. 1 shows the temperature dependence of the main contribution [32] to the heat capacity, the lattice vibrations (red line). The lattice part is described by the Debye function (Eq. 2).

$$C_p(T) \sim \left(\frac{T}{T_D}\right)^3 \int_0^{\frac{\theta_D}{T}} \frac{x^4 e^x}{(e^x-1)^2}\,dx \qquad (2)$$

with $\theta_D \approx 400$.

The heat capacity decreases with the 3rd power of T at low temperatures. The blue line in Fig. 1 is the integrated heat capacity. Between 135K and 10K this function increases by about 50% and between 77K and 10K by 10%, only. Thus, neither the coercivity nor the remanence is the driving force to proceed to temperatures below 77K. On the other hand, the high thermal conductivity of Cu between 10K and 50K may help to reduce thermal gradients in the magnet girder. Furthermore, Holmium which will be discussed later shows the best performance between 4.2K and 10K.

Within a collaboration between SOLEIL and the ESRF the computer program RADIA [33-34] has been extended to simulate the temperature dependence of permanent magnets including the losses due to the spin reorientation. Remanence and coercivity of the magnet supplier is used and the spin-reorientation is included with Eq. 1 using anisotropy constants K1 and K2 from literature. Good agreement between measurement and simulation is documented in [35].

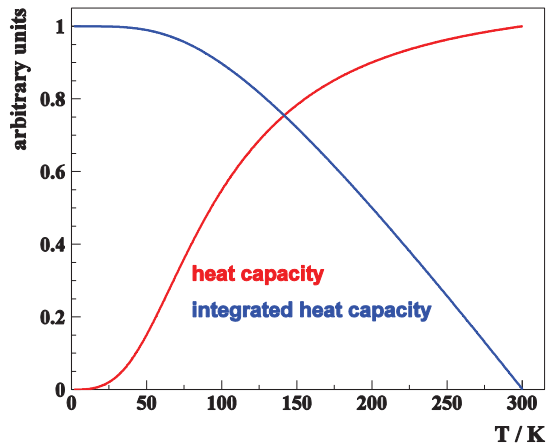

Figure 1: Heat capacity (red) and integrated heat capacity according to Eq. 2. The integration starts from T=300K to show the gain with lowering the temperature.

PRFEB-MAGNETS FOR SHORT PERIOD CRYOGENIC UNDULATORS

Short period undulators are particularly interesting for 2nd harmonic afterburner or laser plasma accelerator based light sources. A 5mm period length room temperature in-vacuum undulator has been built at the Ludwig-Maximilian-Universität Munich (LMU) within an R & D project on table top free electron lasers [36-37], and it was tested at the Mainzer Microtron MAMI [38]. In the next step the design parameters are pushed to higher magnetic fields using an optimized magnet material and an ambitious magnet structure: Within a collaboration of LMU and Helmholtz-Zentrum Berlin (HZB) a new PrFeB grade has been developed by Vacuumschmelze for the use in a small period cryogenic undulator [39]. The material $(Nd_{0.2}Pr_{0.8})_2Fe_{14}B$ has an energy product of $(BH)_{max}$=520 kJ/m^3 at 85K. It has been characterized in a vibrating sample spectrometer between 10 and 300K at HZB [40]. At 10K / 300K the macroscopic properties are B_r=1.7T / 1.41T and H_{cj}=73kOe / 16kOe, respectively. The remanence is lower than the theoretic limit of a perfect crystal with 1.84T / 1.56T (10K / 300K) because the alloy has been optimized to enable an assembly around room temperature.

Using the new PrFeB grade a 20period, 9mm period length, 2.5mm gap prototype undulator has been built [40-41]. So far this grade is fabricated only in small batches and a variation of magnet properties between different batches is unavoidable. A slightly lower coercivity of the undulator material as compared to the material as presented in [39] demanded an assembly in a cold house.

ISBN 978-3-95450-117-5

Meanwhile, the GPD-process has been adapted also to PrFeB. Figure 2 shows three samples of PrFeB magnets with a thickness of 2.2mm before and after GPD. The averaged coercivity enhancement is about 3kOe whereas the remanence remains unchanged. In the future GPD-processed magnets will enable the assembly of high remanence material even at room temperatures.

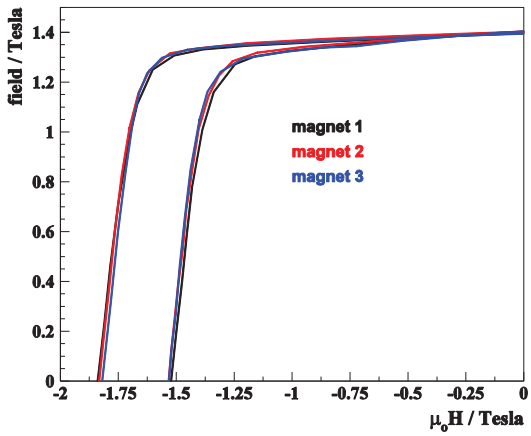

Figure 2: Three samples of PrFeB 2.2mm thick magnets at room temperature before and after a GPD process. The data have been provided by Vacuumschmelze.

The geometric tolerances scale with the period length and on the sub-cm level new fabrication techniques must be explored. The 9mm device was built from a minimum number of high precision mechanic parts. The magnets and poles were placed into precision slots of the magnet girders which define the longitudinal positions. The poles were clamped only from the top (Fig. 3).The accuracy is illustrated by the pole height fluctuation directly after assembly [41]. Only 4 out of 80 poles exceed a band width of ±8μm where the pole heights are defined by the tolerances of three individual parts (girder, poles and pole clamps).

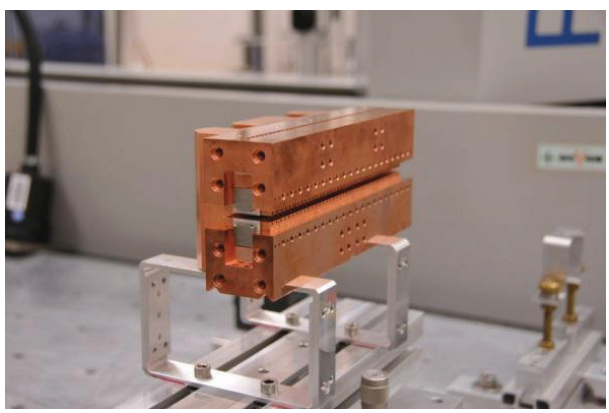

Figure 3: The fixed gap PrFeB-CoFe hybrid undulator as built at HZB. The support structure consists of three parts, the two girders and a backing plate which defines the magnetic gap.

The device has been shimmed by pole height adjustment. In contrast to the European XFEL approach where the poles are moved with screws [42] clamps of different heights are used for this device where the clamps are safely changed after securing the poles without touching the magnets.

The device has been measured with a new in-vacuum Hall probe bench which will be described below. Figure 4 shows the gain in field between 300K and 20K. The measurements and simulations with RADIA agree within 1%. Though, more sophisticated pole designs will be studied in the next chapter the results from the existing design help to establish reliable error bars to the simulations.

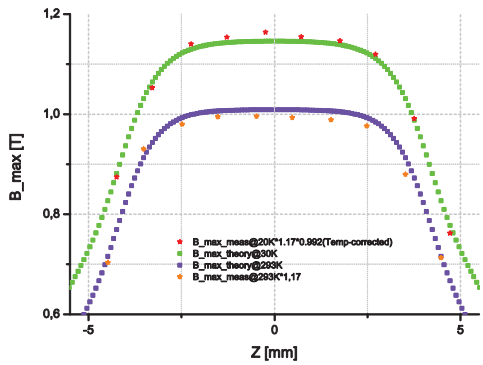

Figure 4: Field measurement at various transverse positions at 300 K and 20K of the 9mm PrFeB HZB / LMU-undulator. The field data are averaged data over the full length of the device. The simulations are based on magnet properties as measured at HZB.

ADVANCED MAGNET DESIGNS

Based on the PrFeB material to be used at 30K a few cases have been simulated to explore the limits of various material combinations for various gaps and period lengths. With sub-cm period lengths all tolerances have to be minimized in order to maximize the effective magnet volume: A TiN coating of 3-4μm thickness is assumed. The dead layer originating from the destruction of the surface grains during final grinding has been fitted from our measurements in a vibrating sample magnetometer to be 8μm, corresponding less than two grain diameters. Other geometric tolerances are assumed to be on the 10μm level. For single pass light sources the transverse good field region is defined only by the transverse extension of the electron beam and the alignment tolerances. Transverse narrow poles can be used and side magnets at the poles pointing with their easy axis to the poles can be implemented [43]. Shaping the poles in transverse direction enhances the field further [44]. We start from a similar pole shape as in [44]. In a first step we simulated a PrFeB / CoFe hybrid undulator. The transverse extension of the pole- tip is 4mm (Fig. 5). The fields achieved for gaps between 0.5 and 2.5mm and periods between 5 and 15mm are plotted in Fig. 6.

ISBN 978-3-95450-117-5

Figure 5: Magnet geometry for simulations. The red blocks are PrFeB magnets pointing to the transversally wedged pole. The blue block is made from CoFe, the brown one from CoFe or Dysprosium or Holmium.

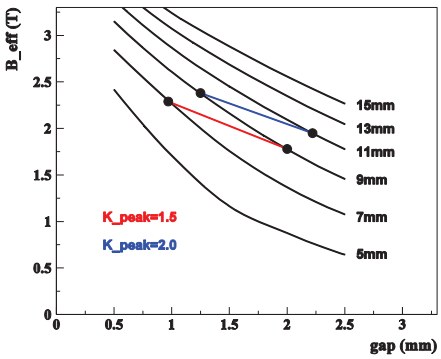

Figure 6: Effective fields at 20K for various period lengths plotted versus the gap. The poles are made from CoFe and are wedged in transverse direction (Fig. 5). The red and blue curves show the period / gap combinations for K=1.5 and K=2.0, respectively.

Tanaka et al discuss a CU plus device, a cryogenic undulator, where the field is enhanced with a high temperature superconducting (HTSC) closed current loop placed around the pole-tip [43,44]. Cooling the device below the critical temperature at nearly zero magnetic gap, and opening the gap, may provide peak fields above the limit of existing SC-NbTi-undulators. With a critical current of 2kA/mm^2 a 14mm period device may produce fields of 1.45 T (2.35 T) at magnetic gaps of 5mm (3mm). Still, extensive R & D in the field of HTSC coils is necessary to fabricate them with reproducible magnet properties and long term stability without degradation.

Low temperatures permit more sophisticated pole designs. At 85K Dy exhibits a phase transition from an antiferromagnetic to a ferromagnetic state [45]. The c-axis of the hexagonal structure is hard whereas the two directions [11-20] and [10-10] in the basal plane, which have a relative angle of 30°, are the soft axes. A single crystal at 10K has saturation magnetizations of 3.815T ([11-20]) and 3.354 T ([10-10]). Mechanic deformation of isotropic polycrystalline Dy (e.g. cold rolling or high pressure extrusion [46]) introduces a texture which causes an anisoptropic magnetic behaviour [47-48]. Commercially available 1.5mm thick rolled Dy-sheets have been characterized at HZB. A maximum saturation magnetization of 3.56T and an asymmetry between the two soft axes in the basal plane of 4.5% have been measured. These data have been used when simulating a hybrid pole where part of the CoFe has been substituted with Dy. The magnet sizes where the same as before. A field increase is noticeable at gaps of 1mm and at period lengths above 10mm. Thus, Dy-pole-tips improve the performance only in the presence of large magnetic fields. The reason is the moderate slope of the BH curve of Dy (Fig. 7). It is well suited for boosting 2-3Tesla dipole magnets or even permanent magnet wigglers further with shaped pole pieces, but it not useful for small period undulator structures.

Holmium shows a steeper slope of the BH-curve at low temperatures (Fig. 7) [48]. In the range of 4.2K-10K the application of a field of 0.1T transforms the helical antiferromagnetic phase into a ferromagnetic phase. Single crystal data at 4.2K [48] have been used in simulations where part of the CoFe at the pole-tip was replaced by Ho. The same parameter space has been explored as before.

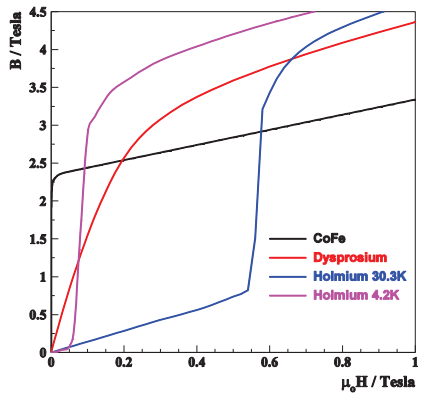

Figure 7: BH curves of various pole materials.

As expected, Ho-pole-tips provide higher fields at 4.2K (Fig. 8). The field gain increases with period length and with 1/gap. For a period length of 10mm the gain with Ho-pole-tips is 10% (15%) for a gap of 1.5mm (1mm).

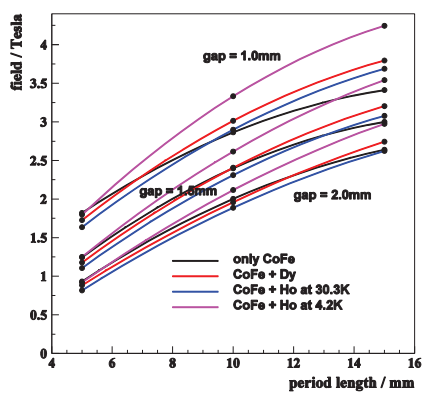

Figure 8: Effective fields at 1, 1.5 and 2mm gap with the same pole geometry as in Figure 6. Data are plotted for pure CoFe and CoFe plus pole-tips of Dy or Ho.

ISBN 978-3-95450-117-5

It is worth mentioning that the magnetic properties of Ho do not change much up to 10K where cryocoolers could be used. Currently, it is not known whether polycrystalline Ho can be oriented by mechanic deformation in similar procedures as Dy. Further R & D on polycrystalline and oriented Ho is required for a thorough evaluation of the applicability to undulators.

MAGNETIC MEASUREMENT TECHNIQUES

Over many years the measurement techniques for undulators have achieved a high level of precision and reliability and they fulfill all requirements for undulator field characterization with respect to spectral properties and accelerator performance. Reducing the period length below 10mm and lowering the gap down to a few mm needs a reconsideration of existing systems. In this regime the pulsed wire technique suffers from dispersion and a sophisticated data processing is essential. Furthermore, wire imperfections get more prominent.

Conventional Hall probe benches cannot be used anymore, thin Hall probes are required for narrow gaps, the alignment tolerances are getting tighter and the systems have to be operated under vacuum conditions and possibly at low temperatures. In the following we will discuss these new aspects.

Pulsed Wire Technique

If a current pulse is sent through a wire located in a transverse magnetic field a wire deflection is imprinted, and it propagates along the wire. It is measured by optical sensors in the field free region. 1st field integrals are derived from short current pulse measurements and 2nd field integrals are derived from a current step function. Choosing the pulse length equal to the undulator period divided by the averaged propagation speed reduces the main signal and enhances the system sensitivity for field errors.

A pulsed wire system is an ideal tool for the characterization of small gap, small period devices, even at cryogenic temperatures. It is vacuum compatible, fits into a small bore and delivers fast and accurate data. Nevertheless, the method has to be applied with care making use of the achievements in signal improvement and data processing over two decades.

In the first papers [50-51] Warren addresses already the parameters which may have an impact on the measurement accuracy: wire sag when measuring long devices, dispersion due to bending stiffness of the wire, signal attenuation for long wires, wave reflections at the wire supports, scattering at wire imhomogeneities, rotation of linear polarization at imperfections, heating and lengthening of the wire and a nonlinearity of the signal. Small signals following the main signals are due to reflections at inhomogeneities whereas small signal arriving before the main signal [52] are due to a coupling of transverse and longitudinal modes which are a factor of 20 faster. This coupling leads also to a rotation of the polarization.

Best results are achieved with a small elastic stiffness, a small wire diameter and a high wire tension, which reduces dispersion and sag (interestingly, the wire sag does not depend on the wire diameter close to the break point). Osmanov et al. discuss the possibility of data correction due to wire sag which allows the measurement of long devices with integrated focusing and additional sextupoles [53].

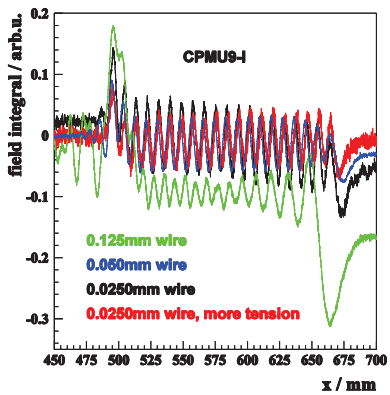

Figure 9: Pulsed wire measurements of the HZB 9mm period PrFeB undulator measured with wires of different thickness. Due to dispersion the signal gets distorted with increasing wire diameter.

The signal quality has been improved significantly over the years using different methods, i) a laser source where the wire obscures the light at the edge of the light cone [54-56] and ii) an infrared light source plus a triangular window [57]. The sensitivities are similar, but the latter source provides a larger linear regime.

Fan et al. used a thick wire (250µm) to reduce the noise from wire imperfections. The increased dispersion is corrected using mathematical methods for unfolding [58]. The dispersion can be measured explicitly with two calibration dipole magnets placed at various distances to the optical sensor. The homogeneous Euler-Bernoulli-Equation (Eq. 3) describes the free propagation of transverse waves within thin rods:

$$\rho A \frac{\partial^2 y}{\partial t^2} - T \frac{\partial^2 y}{\partial z^2} + ED \frac{\partial^4 y}{\partial z^4} = 0; \quad D = \frac{\pi d^4}{64} \qquad (3)$$

I is the current, D the moment of inertia, E the modulus of elasticity, T the tension, ρ the material density, A the area of cross section and d the wire diameter. The Ansatz $y = e^{ik(z-ct)}$ leads to the propagation speed $c(k)$ (Eq. 4) with c_0 being the long wavelength limit.

$$c = c_0 \sqrt{1 + \frac{ED}{T} k^2} \quad \text{with} \quad c_0 = \sqrt{\frac{T}{\rho A}} \qquad (4)$$

Fitting the measured propagation speed $c(k)$ with Eq. 4, the wire parameters can be deduced. Based on these data the inhomogeneous Euler- Bernoulli-Equation – it

ISBN 978-3-95450-117-5

includes the term $B_x(z) \cdot I(t)$ at the right-hand-side of Eq. 3 - can be solved numerically with a self-consistent procedure [59]. The results are independent on the pulse length and they do not show the typical dispersion induced ringing. With this procedure the measurement of small period devices is possible even under vacuum and cryogenic conditions. Finally, the pulsed wire technique is still the only choice for local measurement of fast switching magnets.

In-vacuum Hall probe bench

The on-axis local field distribution as needed for the evaluation of phase errors and in particular the brightness of the higher harmonics cannot be retrieved from pulsed wire data via differentiation of first field integrals since the noise would be too large. The fields can only be measured with a Hall probe scanning along the undulator axis. SCUs have been measured in vertical cryostates with cold Hall probes e.g. [60]. In the meantime horizontal measurement benches for in-vacuum undulators have been developed. Systems have been built at the ESRF [20-21], SPRING-8 [61], SLS and SOLEIL. The benches are less robust than massive granite benches usually used. At ESRF and SOLEIL the tilt of the Hall probe is measured with an interferometer and the data are corrected off-line. In contrast, at SPRING-8 and SLS the measurement system has a feedback implemented, which aligns the bench position with in-air motorized tables. They are connected by several supporting rods to the bench and sealed with bellows. At HZB a 0.5m prototype Hall probe bench has been successfully tested with the 9mm PrFeB undulator. Position as well as yaw and pitch angles of the sledge are measured with an interferometer (Fig. 10). The angles can be corrected on the fly with UHV compatible movers. Based on these experiences HZB will build a 2m Hall probe bench.

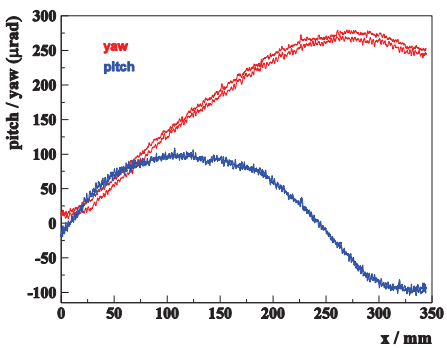

Figure 10: Yaw and pitch of the HZB in-vacuum Hall probe bench. Data have been taken on-the-fly for forward and backward movement.

IMPACT ON MECHANICS

SPRING-8 developed an UHV compatible gap measurement system which has been implemented at the SACLA undulators. At either undulator end a commercial linear encoder is mounted to the upper girder measuring the distance to the lower girder. The system is sealed with bellows [64].

The in-vacuum girders are supported by several rods connected to an outer stiff backing beam. At small gaps only minor differences of the supports may introduce phase errors. SPRING-8 developed a differential screw which permits a fine adjustment of the inner girders for phase error optimization [65]. Either screws of this type or spacers have to be foreseen in small gap devices.

At HZB an optical micrometer has been tested as an alternative gap measurement system suited for cryogenic application. The system does not provide an interface like linear encoders, which can be fed directly into motor controllers. A piece of software as written at HZB communicates with the micrometer and translates the information in a form useful for a feedback operation of the gap motors. A 1-µm positioning accuracy has been demonstrated for this system.

Using modern in-air Hall probe benches 1st and 2nd field integrals can be measured with a higher accuracy than using a pulsed wire system. The accuracy of trajectories from the new in-vacuum Hall probe benches is lower but still comparable to an ultimate pulsed wire system. Nevertheless, the pulsed wire technique is indispensable for small gap in-vacuum devices to cross check with Hall probe data, since a sophisticated calibration procedure is not needed. Moving wire systems suffer from long damping times under vacuum, and they do not provide local information.

CONCLUSION

Small gap small period undulators will be essential components for future light sources. Currently, the shortest undulator period lengths used in 3rd generation storage rings are around 15mm. Undulators in the sub-cm period length regime require a consequent further development of existing devices and measurement tools. Cryogenic devices employing new magnet and pole materials and ambitious pole geometries promise significantly higher fields in the future. These devices have to be measured and tuned carefully to show best performance. New measurement systems have to be developed and existing systems have to be improved. Based on the existing experience the realization of high performing small period devices is possible on a short time scale.

ACKNOWLEDGEMENT

The author thanks F.-J. Boergermann and M. Katter, Vacuumschmelze, for providing the measurements on the grain boundary diffused samples, M. Scheer for the magnetic field simulations, C. Kuhn for the interferometric data of the in-vacuum bench and A. Gaupp for the Dy-data and many fruitful discussions.

REFERENCES

[1] S. Sasaki, Nucl. Instr. Meth. A347 (1994) 83-86.

ISBN 978-3-95450-117-5

[2] J. Chavanne et al, Proc. of EPAC Stockholm, Sweden (1998) 2213-2215.
[3] B. Diviacco et al, Proc. of EPAC Stockholm, Sweden (1998) 2216-2218.
[4] C. Steier et al., Proc. of EPAC Edinburgh, Scotland (2008) 2311-2313.
[5] S. Casalbuoni et al., Phys. Rev. ST Accel. Beams 9, 010702 (2006).
[6] C. Boffo et al., Proc. of FEL Conference, Malmoe, Sweden (2010) 660-663.
[7] E. Moog et al., Proc. of IPAC Kyoto, Japan (2010) 3198-3200.
[8] S. Prestemon et al., Proc. of PAC Vancouver, BC, Canada (2009) 2438-2440.
[9] J. Bahrdt et al., Proc. of FEL Conference, Trieste, Italy (2004) 610-613.
[10] A. Temnykh, Phys. Rev. ST Accel. Beams, 11, 120702 (2008) 1-10.
[11] W. Rodewald et al., Trans. Magn. 36 (2000) 3279-3281.
[12] private communication, Vacuumschmelze, Hanau, Germany (20011).
[13] W. F. Brown, Jr., Rev. of Mod. Phys. 17 (1945) 15.
[14] H. Kronmüller, Phys. Stat. Sol., B 144 (1987) 385-396.
[15] K. Uestuener, M. Katter, W. Rodewald IEEE Trans. Magn. 42 (2006) 2897.
[16] K. Park et al., Proceedings of 16th Int. Workshop on RE Magnets and their Applications, Sendai, Japan (2000) 257.
[17] H. Nakamura et al., J. Phys. D: Appl. Phys. 44 (2011) 064004-1-5.
[18] T. Schmidt et al. Proc. of the FEL Conference, Liverpool, United Kingdom (2009) 706-718.
[19] T. Hara et al., Phys. Rev. Special Topics Accel. Beams 7 (2004) 050702.
[20] K.-D. Durst, Jou. of Magnetism and Magnetic Materials 59 (1986) 86-94.
[21] C. Kitegi et al., Proc. of EPAC, Edinburgh Scotland (2006) 3559-3561.
[22] J. Chavanne et al., Proc. of EPAC, Genoa, Italy (2008) 2243-2245.
[23] T. Tanabe et al., AIP Conf. Proc. 879 (2006) 283.
[24] SLS T. Tanaka et al., Phys. Rev Special Topics Acc. and Beams, 12, 120702 (2009) 1-5.
[25] C.W. Ostenfeld et al., Proc. of IPAC, Kyoto, Japan (2010) 3093-3095.
[26] SOLEIL C. Benabderrahmane et al., Proc. of EPAC, Genoa, Italy (2008) 2225-2227.
[27] G. Le Bec, et al., Proc of PAC, Vancouver, BC, USA (2009) 327-329.
[28] C. Benabderrahmane et al., Proc. of IPAC, Kyoto, Japan (2010) 3096-3098.
[29] T. Tanabe et al., AIP Conf. Proc., SRI 2009 Melbourne, Australia, Vol. 1234 (2010) 29-32.
[30] P. Colomp, et al., Machine Technical Note 1-1996/ID, 1996.
[31] M. Petra et al., Nucl. Instr. and Meth. in Phys. Res. A, 507 (2003) 422-425.
[32] H. Fujii et al., Jou. of Magnetism and Magnetic Material 70 (1987) 331-333.
[33] O. Chubar et al., J. of Sync. Rad. 5 (1998) 481-484.
[34] P. Elleaume et al., Proc. of the PAC, Vancouver, BC, Canada (1997) 3509-3511.
[35] G. Le Bec et al., Proc. of PAC, Vancouver, BC, Canada (2009) 327-329.
[36] F. Grüner et al., Appl. Physics B 8 (2007) 431-435.
[37] T. Eichner et al., Phys. Rev. Spec. Topic. AB, **10**, 082401 (2007) 1-9.
[38] M. Fuchs et al., Nature Physics, 5 (2009) 826-829.
[39] K. Üstüner et al., 20th Conference on Rare Earth Permanent Magnets, Crete 2008.
[40] J. Bahrdt et al., AIP Conf. Proc., SRI 2009 Melbourne, Australia, Vol. 1234 (2010) 499-502.
[41] J. Bahrdt et al., Proc. of IPAC, Kyoto, Japan (2010) 3111-3113.
[42] J. Pflüger et al., Nucl. Instr. and Meth. in Phys. Res. A429 (1999) 368.
[43] T. Tanaka et al., Phys. Rev. Special Topics AB, Vol. 7, 090704 (2004) 1-5.
[44] T. Tanaka et al. New J. Phys., 8 (2006) 287.
[45] D. R. Berendt et al., Phys. Rev. 109 (1958) 1544.
[46] V. Stepankin, Physica B 211, 345-347 (1995).
[47] R. H. Hopkins, Metall. Trans. 5 (1974) 1183.
[48] W. M. Swift et al., IEEE Trans. on Magnetics 10 (1974) 308.
[49] W.C. Koehler et al., Physical Review, Vol. 158, No 2 (1967) 450-461.
[50] R. W. Warren, Nucl. Instr. and Meth. in Phys. Res. A 272 (1988) 257-263.
[51] R. W. Warren et al., "Undulator Magnets for Synchrotron Radiation and Free Electron Lasers", Proc. Adriatico Res. Conf., Trieste, Italy, June 1987, eds. R. Bonifacio, L. Fonda, C. Pellegrini (World Scientific, 1988) p28.
[52] O. Shahal et al., Nucl. Instr. and Meth. in Phys. Res. A 296 (1990) 588.
[53] N.S. Osmanov et al., Nucl.Instr. and Meth. in Phys. Res. A 407 (1998) 443-447.
[54] A.A. Varfolomeev et al., Nucl. Instr. and Meth. in Phys. Res. A 359 (1995) 93-96.
[55] D.W. Preston, R. W. Warren, Nucl. Instr. and Meth. in Phys. Res. A 318 (1992) 794-797. 818-821.
[56] R.W. Warren, D. W. Preston, Nucl. Instr. and Meth. in Phys. Res. A 318 (1992) 818-821.
[57] Varfolomeev et al., Nucl. Instr. and Meth. in Phys. Res. A 341 (1994) 470-472.
[58] T.C. Fan et al., Proc of PAC, Chicago, Il, USA (2001) 2775-2777. T.C. Fan et al., Rev. of Sci. Instr., Vol. 73, No 3 (2002) 1430-1432.
[59] D. Arbelaez, Workshop on small period undulators, Berkeley June, 2011.
[60] E. Mashkina et al., IEEE Trans. App. Supercond., Vol.18, No 2 (2008) 1637-1640.
[61] T. Tanaka et al., Proc. of FEL Conference, Gyeongju, South Korea (2008) 371-374.
[62] T. Tanaka, Proc. of IPAC, Kyoto, Japan (2010) 3147-3149.

ISBN 978-3-95450-117-5